INTERNATIONAL JOURNAL OF MARITIME TECHNOLOGY

IJMT Vol.2/ Summer 2014 (67-74)

Available online at: http://ijmt.ir/browse.php?a_code=A-10-264-1&sid=1&slc_lang=en

TECHNICAL NOTE

Buckling Analysis of Panels and Comparative Study on ABS and DNV Rules

Reza Akbari Alashti[1], Seyyed Ali Ahmadi[2]

[1] *Associate Professor, Department of Mechanical Eng, Babol University of Technology; raalashti@hotmail.com*
[2] *M.Sc. Graduate, Department of Mechanical Eng, Babol University of Technology; ali_ahmadi1366@yahoo.com*

ARTICLE INFO

Article History:
Received: 5 Jan. 2013
Accepted: 11 Mar. 2014
Available online: 22 Sep. 2014

Keywords:
differential quadrature method,
buckling,
offshore structure,
curved panel,
classification society

ABSTRACT

In this study, buckling analysis of panel types of marine and offshore structural components with initial imperfection under the combined action of lateral pressure and axial compression is carried out. The governing differential equations for thin and moderately thick shells are developed in terms of components of the displacement field. The governing ordinary differential equations are then discretized and reduced to a linear system of homogeneous equations employing the differential quadrature method. The results obtained by the present method are verified with results obtained by finite element method and those reported in the literature. Design rules of two classification societies, namely American Bureau of Shipping (ABS) and Det Norske Veritas (DNV) are briefly presented and results are compared with rules requirements of these societies. It is observed that DNV rules are more conservative than ABS rules for calculation of buckling loads of marine and offshore structures. Effects of several parameters including the curvature, initial imperfection, geometric ratios and loading conditions on the buckling behavior of a cylindrical shell and a curved panel are investigated.

1. Introduction

Cylindrical shells and panels are common structural components in various types of marine, offshore and subsea structures. The widespread use of these structures in marine industry has encouraged several researches on the stability and failure analysis of these components and development of failure prevention methods. In the past and mainly due to lack of knowledge about the buckling phenomenon, ultimate strength was considered as the main design factor for marine structures. Now, by having done studies and researches on buckling behavior of structures, buckling strength has been regarded as the main factor in designing of shell structures.

Since, several unexpected conditions may exist for offshore structures in marine environment, it is necessary to design these structures with higher level of safety. Imperfections are one of these unexpected conditions. The buckling strength of an offshore structural component is highly related to the amplitude and shape of the imperfections which are mainly produced during manufacturing, storage, transportation, installation processes or caused by corrosion pitting. Testing of a corroded member indicated that even nominal values of corrosion resulted in a lost load carrying capacity of up to 35% to 50% [1]. Therefore, special care should be taken in the buckling and ultimate strength assessments of corroded components in order to ensure that these structures are within acceptable level of safety. In the context of offshore design, the structural components are mainly made of steel and due to the method of fabrication, they may possess considerable inherent initial imperfections and residual stresses. Therefore, it is necessary to consider many other important factors such as collapse and post buckling modes and likely failure modes in general buckling analysis. Two types of formulations are basically considered namely the lower bound and the mean value [2]. The governing design equations for buckling strength assessment of shells related to marine structures are the rules requirements set by marine classification societies, e.g. American Bureau of Shipping (ABS) and Det Norske Veritas (DNV). DNV formulation can be considered as a lower bound one and characterised by the under prediction of the strength of offshore structures. The ABS rules for building and classing offshore installations [3], mobile offshore drilling units [4], and steel vessels [5], require that buckling strength be provided for the structure as a whole and for each structural member.

On the other hand, Mirfakhraei *et al.* studied the buckling behavior of tanks under seismic loading condition [6]. Buckling of long shells under three point bending was investigated by Redekop *et al.* [7]. Mirfakhraei and Redekop [8] used the differential quadrature method to study the buckling behavior of circular cylindrical shells. Shen and Chen [9-10] investigated the buckling behavior of cylindrical shells under the action of axial compression and lateral pressure using the boundary layer theory that was found to be very cumbersome in mathematical calculations for practical applications.

In this study, three dimensional stability equations of the shell are developed on the basis of the second Piola–Kirchhoff stress tensor. The shell is assumed to be subjected to a combination of axial compression and lateral pressure loadings. The differential quadrature method is used to discretize the differential equations and to obtain the buckling load of thin cylindrical shells and panels. Numerical results are compared with finite element solutions and results reported in the literature. Effects of various parameters including the panel curvature, mechanical loading combinations and geometric ratios on the buckling load of the panel are investigated. The novelty of the present work is to obtain a benchmark solution for the critical buckling load of cylindrical shells. The main objective of the work is to present a new set of three dimensional formulations for buckling of the panel bounded by stiffeners and compare results with DNV and ABS rules for different cases of load conditions. Furthermore, we have tried to show similarities and differences in the prediction of the limit state by these two rules.

2. Formulation of the problem

A curved panel of length L, width S, curvature angle β, mid-surface radius a, and variable thickness $h(x)$ is considered. The geometry and the coordinate system (r, θ, x) of the panel are shown in Figure 1.

It is assumed that the shell has an axisymmetric and periodic imperfection in the axial direction and the thicknesses of the shell obey the following formula:

$$h(x) = h_0(1 - \varepsilon \cdot \cos\frac{\pi}{L}(x - \frac{L}{2})) \qquad (1)$$

Where h_0 is the thickness of a perfect cylindrical shell and ε is the non-dimensional parameter of imperfection. According to the presented formulation, the mid-surface radius $a(x)$ varies in the axial direction while the inner radius R_1 is assumed to be constant. The thicknesses of the shell at two ends of the shell are the same for all values of ε, *i.e.* $h(x)=h_0$ at $x=0,L$ and $h(x)=h_0(1-\varepsilon)$ at $x=L/2$.

The corresponding displacement functions at the perturbed position for the buckling state are expressed as:

$$\begin{aligned} w(r,\theta,x) &= w^0(r,\theta,x) + \alpha \cdot w'(r,\theta,x) \\ v(r,\theta,x) &= v^0(r,\theta,x) + \alpha \cdot v'(r,\theta,x) \\ u(r,\theta,x) &= u^0(r,\theta,x) + \alpha \cdot u'(r,\theta,x) \end{aligned} \qquad (2)$$

Where α is an infinitesimally small quantity; $w^0(r,\theta,x)$, $v^0(r,\theta,x)$ and $u^0(r,\theta,x)$ denote initial values of components of displacement field and $w'(r,\theta,x)$, $v'(r,\theta,x)$ and $u'(r,\theta,x)$ denote values of components of displacement field in the disturbed position in the radial, circumferential and axial directions, respectively.

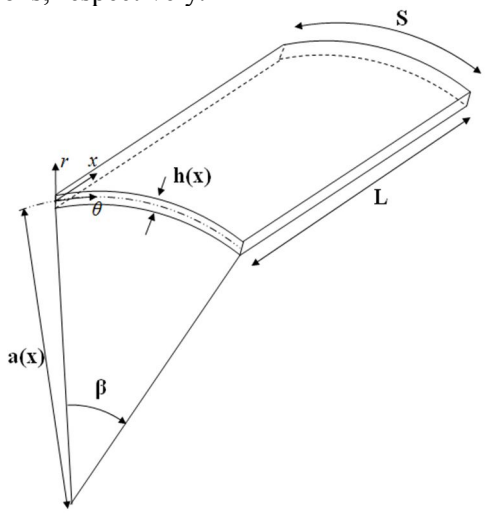

Figure 1. Panel geometry and coordinates

The stress-strain relations for an isotropic material are defined as:

$$\begin{aligned} &\sigma_{rr} = (2G+\lambda)\varepsilon_{rr} + \lambda(\varepsilon_{\theta\theta} + \varepsilon_{xx}),\ \tau_{r\theta} = G\varepsilon_{r\theta} \\ &\sigma_{\theta\theta} = (2G+\lambda)\varepsilon_{\theta\theta} + \lambda(\varepsilon_{xx} + \varepsilon_{rr}),\ \tau_{rx} = G\varepsilon_{rx} \\ &\sigma_{xx} = (2G+\lambda)\varepsilon_{xx} + \lambda(\varepsilon_{\theta\theta} + \varepsilon_{rr}),\ \tau_{x\theta} = G\varepsilon_{x\theta} \end{aligned} \qquad (3)$$

Where λ and G are the Lame coefficients:

$$G(z) = \frac{E(z)}{2(1+\upsilon)},\ \lambda(z) = \frac{E(z)\cdot\upsilon}{(1+\upsilon)(1-2\upsilon)} \qquad (4)$$

By substituting parameters of Eq. (2) into the linear strain-displacement equations and using Eq. (3), strain and stress components in the perturbed configuration can be obtained in terms of components of the displacement field.

Equations of equilibrium are written in terms of the second Piola–Kirchhoff stress tensor σ, in following form [11]:

$$div(\sigma \cdot F^T) = 0,\ F = I + rgad\vec{V} \qquad (5)$$

Where F is the deformation gradient, $\vec{V}$ is the displacement vector and I is the unit tensor. For a three dimensional problem, Eq. (5) can be expanded in the radial, circumferential and axial directions.

Considering linear normal strains $\varepsilon_{ij} = \varepsilon_{ij}^0 + \alpha \cdot \varepsilon_{ij}'$ and rotations $\omega_{ij} = \omega_{ij}^0 + \alpha \cdot \omega_{ij}'$, as well as stresses and keeping the linear terms in α, a set of equations for the perturbed state is developed. The shear strain, shear stress and rotation are assumed to be zero in the initial condition, hence the corresponding terms are dropped from the equilibrium equations. Since, the non-zero normal strains are assumed to be much smaller than 1, *i.e.* $(1+e_{rr}^0 \approx 1,\ 1+e_{\theta\theta}^0 \approx 1,\ 1+e_{xx}^0 \approx 1)$, a system of homogeneous differential equations are obtained which are linear in derivatives of *w, v , u* with respect to *r,* θ and *x* .

$$\frac{\partial}{\partial r}\left(\sigma_{rr}^0 \varepsilon_{rr}' + \sigma_{rr}'\right) + \frac{\partial}{\partial x}\left(\tau_{rx}' + \sigma_{xx}^0 (\varepsilon_{rx}' + \omega_{rx}')\right)$$
$$+\frac{1}{r}\frac{\partial}{\partial \theta}(\tau_{r\theta}' + \sigma_{\theta\theta}^0(\varepsilon_{r\theta}' + \omega_{r\theta}')) \qquad (6a)$$
$$+\frac{1}{r}\left(\sigma_{rr}' + \sigma_{rr}^0 \varepsilon_{rr}' - \sigma_{\theta\theta}' - \sigma_{\theta\theta}^0 \varepsilon_{\theta\theta}'\right) = 0$$

$$\frac{\partial}{\partial r}\left(\tau_{r\theta}' + \sigma_{rr}^0(\varepsilon_{r\theta}' - \omega_{r\theta}')\right) + \frac{1}{r}\frac{\partial}{\partial \theta}\left(\sigma_{\theta\theta}^0 \varepsilon_{\theta\theta}' + \sigma_{\theta\theta}'\right)$$
$$+\frac{\partial}{\partial x}\left(\tau_{\theta x}' + \sigma_{xx}^0(\varepsilon_{\theta x}' - \omega_{\theta x}')\right) \qquad (6b)$$
$$+\frac{1}{r}\left(\sigma_{rr}^0(\varepsilon_{r\theta}' - \omega_{r\theta}') + 2\tau_{r\theta}' + \sigma_{\theta\theta}^0(\varepsilon_{r\theta}' + \omega_{r\theta}')\right) = 0$$

$$\frac{\partial}{\partial r}\left(\tau_{rx}' + \sigma_{rr}^0(\varepsilon_{rx}' - \omega_{rx}')\right) + \frac{\partial}{\partial x}\left(\sigma_{xx}' + \sigma_{xx}^0 \varepsilon_{xx}'\right)$$
$$+\frac{1}{r}\frac{\partial}{\partial \theta}\left(\sigma_{\theta\theta}^0(\varepsilon_{\theta x}' + \omega_{\theta x}') + \tau_{\theta x}'\right) \qquad (6c)$$
$$+\frac{1}{r}\left(\tau_{rx}' + \sigma_{rr}^0(\varepsilon_{rx}' - \omega_{rx}')\right) = 0$$

3. Boundary conditions

Boundary conditions of the shell are defined with the help of equilibrium equations using the second Piola – Kirchhoff tensor σ as:

$$(F \cdot \sigma) \cdot \vec{n} = \vec{t} \qquad (7)$$

Where $\vec{t}$ is the traction vector and $\vec{n}$ is the outward pointing unit normal vector. Applying the boundary condition as defined in Eq. (7) for the initial and perturbed equilibrium positions, the following relations for stress components at the lateral surface are obtained:

$$\sigma_{rr}'\left(a+\frac{h}{2},\theta\right) = \sigma_{rr}'\left(a-\frac{h}{2},\theta\right) = 0,$$
$$\tau_{r\theta}'\left(a+\frac{h}{2},\theta\right) = \tau_{r\theta}'\left(a-\frac{h}{2},\theta\right) = 0, \qquad (8)$$
$$\tau_{rx}'\left(a+\frac{h}{2},\theta\right) = \tau_{rx}'\left(a-\frac{h}{2},\theta\right) = 0$$

The stress components σ_{rr}^0 and $\sigma_{\theta\theta}^0$ at the outer and inner lateral surfaces of the shell due to the action of the lateral pressure *p*, are given by the well known expressions from the linear elasticity theory [12]:

$$\sigma^0{}_{\theta\theta} = -p\left[1+\left(\frac{R1}{r}\right)^2\right]\cdot\left[1-\left(\frac{R1}{R2}\right)^2\right]^{-1} = f_{\theta\theta}\cdot p,$$
$$\sigma^0{}_{rr} = -p\left[1-\left(\frac{R1}{r}\right)^2\right]\cdot\left[1-\left(\frac{R1}{R2}\right)^2\right]^{-1} = f_{rr}\cdot p \qquad (9)$$

Since in the present work we consider curved panels between adjacent pairs of ring and stringers stiffeners, simply supported boundary conditions are defined for panel edges:

$$w = u = v = 0 \qquad at \quad x = 0, L$$
$$w = u = v = 0 \qquad at \quad \theta = 0, \beta \qquad (10)$$

4. Buckling load calculation

Equations which are developed in the previous section include rotation and strain terms and can be used for general shells. Substituting components of the displacement filed into linear strain-displacement equations and applying the stress-strain relations i.e. Eq. (3), components of the stress field are defined in terms of components of the displacement field. Finally, by substituting the resulted expression in Eq. (6), the equilibrium equations in the buckled state are defined in terms of components of the displacement field.

In the present study, a semi-analytical method called the differential quadrature method is used to discretize and solve the governing buckling equations. This method suggests that the first order derivative of the function *f(x)* can be approximated as a linear sum of all functional values in the domain:

$$\left.\frac{df}{dx}\right|_{x=x_i} = \sum_{j=1}^{N} w_{ij}^{(1)} \cdot f(x_j)$$
$$for\ i = 1, 2, ..., N \qquad (11)$$

Where $w^{(1)}_{ij}$ is the weighting coefficient and *N* denotes the number of grid points in the domain. It should be noted that the weighting coefficients are different for different grid points, x_i. The polynomial and Fourier expansion methods are commonly used to determine the weighting coefficients. In this study, the polynomial expansion based differential quadrature is used to approximate the first and second order derivations in the radial and the longitudinal directions [13].

Now, using unequal spacing scheme for sampling points in the domain and applying differential quadrature method for governing equations, we have:

$$
\begin{aligned}
&(2G+\lambda)\sum_{n=1}^{N}a_{k,n}^{(2)}w_{i,j,n}+\frac{(2G+\lambda)}{r}\sum_{n=1}^{N}a_{i,n}^{(1)}w_{n,j,k}\\
&+(G+\lambda)\sum_{n=1}^{N}\sum_{m=1}^{Q}a_{i,n}^{(1)}b_{j,m}^{(1)}w_{n,m,k}-\frac{(2G+\lambda)}{r^2}w_{i,j,k}\\
&+\frac{(G+\lambda)}{r}\sum_{n=1}^{N}\sum_{m=1}^{M}c_{k,m}^{(1)}a_{i,n}^{(1)}v_{n,j,m}-\frac{(3G+\lambda)}{r^2}\sum_{n=1}^{M}c_{k,n}^{(1)}v_{i,j,n}\\
&-\frac{G}{r^2}.\sum_{n=1}^{Q}c_{k,n}^{(2)}w_{i,j,n}+\frac{F}{\pi.r^2.\left(R_2^2-R_1^2\right)}\sum_{n=1}^{Q}b_{j,n}^{(2)}w_{i,n,k}\\
&+G.\sum_{n=1}^{Q}b_{j,n}^{(2)}w_{i,n,k}+P\left[\frac{df_{rr}}{dr}\sum_{n=1}^{N}a_{i,n}^{(1)}w_{n,j,k}\right.\\
&+f_{rr}\sum_{n=1}^{N}a_{i,n}^{(2)}w_{n,j,k}+\frac{f_{rr}}{r}\sum_{n=1}^{N}a_{i,n}^{(1)}w_{n,j,k}\\
&\left.-\frac{2f_{\theta\theta}}{r^2}\sum_{n=1}^{M}c_{n,k}^{(1)}v_{i,j,n}-\frac{f_{\theta\theta}}{r^2}\left(w_{i,j,k}-\sum_{n=1}^{M}c_{k,n}^{(2)}w_{i,j,n}\right)\right]=0
\end{aligned}
\tag{12a}
$$

$$
\begin{aligned}
&G.\sum_{n=1}^{N}a_{i,n}^{(2)}v_{n,j,k}+\frac{(G+\lambda)}{r}\sum_{n=1}^{N}\sum_{m=1}^{M}c_{k,m}^{(1)}a_{i,n}^{(1)}w_{n,j,m}\\
&+\frac{(3G+\lambda)}{r^2}\sum_{n=1}^{M}c_{k,n}^{(1)}w_{i,j,n}+G.\sum_{n=1}^{Q}b_{j,n}^{(2)}v_{i,n,k}\\
&-\frac{G}{r^2}v_{i,j,k}+\frac{(G+\lambda)}{r}\sum_{n=1}^{Q}\sum_{m=1}^{M}c_{k,m}^{(1)}b_{j,n}^{(1)}u_{i,n,m}\\
&+\frac{(2G+\lambda)}{r^2}\sum_{n=1}^{M}c_{j,n}^{(2)}v_{i,n,k}+\frac{G}{r}\sum_{n=1}^{N}a_{i,n}^{(1)}v_{n,j,k}\\
&+\frac{F}{\pi.r^2.\left(R_2^2-R_1^2\right)}\sum_{n=1}^{Q}b_{j,n}^{(2)}v_{i,n,k}+P\left[\frac{df_{rr}}{dr}\sum_{n=1}^{N}a_{i,n}^{(1)}v_{n,j,k}\right.\\
&+f_{rr}\sum_{n=1}^{N}a_{i,n}^{(2)}v_{n,j,k}+\frac{f_{rr}}{r}\sum_{n=1}^{N}a_{i,n}^{(1)}v_{n,j,k}\\
&\left.+\frac{2f_{\theta\theta}}{r^2}\sum_{n=1}^{M}c_{k,n}^{(1)}w_{i,j,n}-\frac{f_{\theta\theta}}{r^2}\left(v_{i,j,k}-\sum_{n=1}^{M}c_{k,n}^{(2)}v_{i,j,n}\right)\right]
\end{aligned}
\tag{12b}
$$

$$
\begin{aligned}
&G.\sum_{n=1}^{N}a_{i,n}^{(2)}u_{n,j,k}+\frac{G}{r}\sum_{n=1}^{N}a_{i,n}^{(1)}u_{n,j,k}\\
&+(G+\lambda)\sum_{n=1}^{N}\sum_{m=1}^{Q}a_{i,n}^{(1)}b_{j,m}^{(1)}w_{n,m,k}\\
&+(2G+\lambda)\sum_{n=1}^{Q}b_{j,n}^{(2)}v_{i,j,k}\\
&+\frac{(G+\lambda)}{r}\sum_{n=1}^{Q}\sum_{m=1}^{M}b_{j,n}^{(1)}c_{k,m}^{(1)}v_{i,n,m}\\
&+\frac{(G+\lambda)}{r}\sum_{n=1}^{Q}b_{j,n}^{(1)}w_{i,n,k}+\frac{G}{r^2}\sum_{n=1}^{N}a_{i,n}^{(2)}u_{n,j,k}\\
&+\frac{F}{\pi.r^2.\left(R_2^2-R_1^2\right)}\sum_{n=1}^{Q}b_{j,n}^{(2)}u_{i,n,k}\\
&+P\left[\frac{df_{rr}}{dr}\sum_{n=1}^{N}a_{i,n}^{(1)}u_{n,j,k}+f_{rr}\sum_{n=1}^{N}a_{i,n}^{(2)}u_{n,j,k}\right.\\
&\left.+\frac{f_{\theta\theta}}{r^2}\sum_{n=1}^{M}c_{k,n}^{(2)}u_{i,j,n}+\frac{f_{rr}}{r}\sum_{k=1}^{N}a_{i,n}^{(1)}u_{n,j,k}\right]
\end{aligned}
\tag{12c}
$$

Where $a^{(k)}_{ij}$, $b^{(k)}_{ij}$ and $c^{(k)}_{ij}$ denote weighting coefficients of the k^{th} order derivative in the r, x and θ-direction, respectively; N, Q and M are grid point numbers in the r, x and θ- direction, respectively.

For simplicity and ease of calculation, the perturbed displacement can be written in the periodic form for some specific boundary conditions. For example, considering simply supported condition for longitudinal edges, we have:

$$
\begin{aligned}
w(r,\theta,x)&=B(r,x)\cdot\sin\left(\frac{m\pi}{\beta}\theta\right)\\
v(r,\theta,x)&=A(r,x)\cdot\cos\left(\frac{m\pi}{\beta}\theta\right)\\
u(r,\theta,x)&=C(r,x)\cdot\sin\left(\frac{m\pi}{\beta}\theta\right)
\end{aligned}
\tag{13}
$$

Where m is the circumferential half buckling mode number.

The critical value of the external pressure, P_{cr}, *i.e.* the buckling load, is calculated by solving the set of equations which are transformed into the standard eigenvalue equation of the following form:

$$
\begin{aligned}
&(-[DBG][BB]^{-1}[BD]+[DDG])^{-1}\\
&*(-[DB][BB]^{-1}[BD]+[DD])[u\quad v\quad w]^{T}\\
&-P[\mathrm{I}][u\quad v\quad w]^{T}=0
\end{aligned}
\tag{14}
$$

Where sub-matrices *[BB], [BD]* and *[DBG], [DD], [DB], [DDG]* are resulted from the boundary conditions and governing equations, respectively.

In order to compare buckling loads of cylindrical shells and curved panels obtained by the present method and those obtained by design rules set by classification societies, a brief explanation about these rules is given.

According to DNV rules, the stability requirement for shells subjected to one or more loads is given by:

$$
\sigma_{j,sd}\le f_{ksd} \tag{15}
$$

Where $\sigma_{j,sd}$ is the design equivalent von Misses stress that is obtained by membrane stresses created by axial, circumferential, bending and shear loading and f_{ksd} is the design buckling strength which is defined as:

$$
f_{ksd}=\frac{f_{ks}}{\gamma_M} \tag{16}
$$

The characteristic buckling strength of shells, f_{ks} , is obtained by:

$$
f_{ks}=\frac{f_y}{\sqrt{1+\bar{\lambda}_s^{\,4}}} \tag{17}
$$

where f_y is yield strength of the material. The material factor, γ_M is given as:

$$\begin{aligned} \gamma_M &= 1.15 && \bar{\lambda}_s < 0.5 \\ \gamma_M &= 0.85 + 0.6\bar{\lambda}_s && 0.5 \le \bar{\lambda}_s \le 1 \\ \gamma_M &= 1.45 && \bar{\lambda}_s > 1 \end{aligned} \quad (18)$$

In above, $\bar{\lambda}_s$ is obtained by design stresses and elastic buckling strengths of curved panels and circular cylindrical shells subjected to different loading conditions [14]. In this work, buckling behavior of unstiffened or ring-stiffened circular cylindrical shells and unstiffened curved panels or panels bounded by two adjacent stiffeners are investigated. Therefore, cylindrical shell components with $L/s<1$ and panels with $L/s>1$ are considered. Elastic buckling stress for cylindrical shells and curved panels are defined in Eq.s (19) and (20), respectively.

$$f_E = C\frac{\pi^2 E}{12(1-\nu^2)}\left(\frac{h}{L}\right) \quad (19)$$

$$f_E = C\frac{\pi^2 E}{12(1-\nu^2)}\left(\frac{h}{s}\right) \quad (20)$$

where C is the reduced buckling coefficient:

$$C = \Psi\sqrt{1+\left(\frac{\rho\xi}{\Psi}\right)^2} \quad (21)$$

where ρ, ψ and ξ are buckling coefficients which are dependent on the loading conditions.

According to ABS rules, critical buckling stress for unstiffened cylindrical shells subjected to external pressure may be defined as:

$$\sigma_{C\theta R} = \Phi\sigma_{E\theta R} \quad (22)$$

Where Φ is the plasticity reduction factor and $\sigma_{E\theta R}$ is the elastic hoop buckling stress and defined as:

$$\sigma_{E\theta R} = \rho_{\theta R}\frac{q_{CE\theta R}(a+0.5h)}{h}K_\theta \quad (23)$$

In above equation, $\rho_{\theta R}$ is the lower bound knock-down factor, K_θ is a coefficient to account for the effect of the ring stiffener and elastic buckling stress, $q_{CE\theta R}$ is a function of E, h, a, υ and L [15]. For the axial loading case the same set of equations are applied.

5. Numerical results

In this study, material properties of the shell are assumed to be isotropic. The material properties of the shell i.e. the Young's modulus E, and the Poisson's ratio, υ are assumed to be 200 GPa and 0.3, respectively.

At first, accuracy of the presented method is validated against results reported in the literature. The normalized results of stability equations for an isotropic moderately thick cylindrical shell under the action of pure axial compression obtained by differential quadrature method are presented in Table 1. For this specific case the Young's modulus E, of the shell is considered to be 14 GPa. The results are validated against the results reported by Kardomateas [16], Timoshenko [17] and Flugge [18]. It is observed from the table that results are in good agreement with reported results for moderately thick shells. The results for buckling loads of a thin perfect cylindrical shell under the lateral pressure are presented in Table 2 that indicates a good agreement with finite element solutions, however the difference between presented results and those reported by Mirfakhraei increases as the ratio L/a increases or a/h decreases.

Also buckling mode shapes obtained by Ansys software for complete shells with $a/h=300$ and different values of L/a are presented in Figure 2. It can be seen that buckling modes in circumferential direction have periodic form as considered in relations (13).

Table 1. Critical pure axial compression load of a cylindrical shell
E=14* GPa, *ν=0.3*, R_2=1 m, *L/R_2=5* Critical Load*:
$f = FR_2/\pi Eh(R_2^2 - R_1^2)$

R_2/R_1	Present	Ref. [16]	Ref. [17]	Ref. [18]
1.05	0.4334	0.4426 (2,1)	0.4348 (2,1)	0.4525 (2,1)
1.10	0.3739	0.3910 (2,1)	0.3865 (2,1)	0.4019 (2,1)
1.15	0.4158	0.4547 (2,1)	0.4373 (2,2)	0.4710 (2,1)
1.20	0.4088	0.4371 (2,2)	0.4184 (2,2)	0.4620 (2,2)

Table 2. Critical pure lateral pressure (kPa) of a clamped-clamped cylindrical shell
E=200* GPa, *ν=0.3

L/a	a/h	m	Mirfakhraei [8]	FEM	Present	% error
1	300	13	166.54	159.77	175.03	2.18
	500	15	46.993	43.67	54.48	1.53
	1000	18	8.415	8.04	10.45	0.93
2	300	9	84.79	79.84	88.134	3.15
5	300	6	32.9	29.45	35.76	5.11

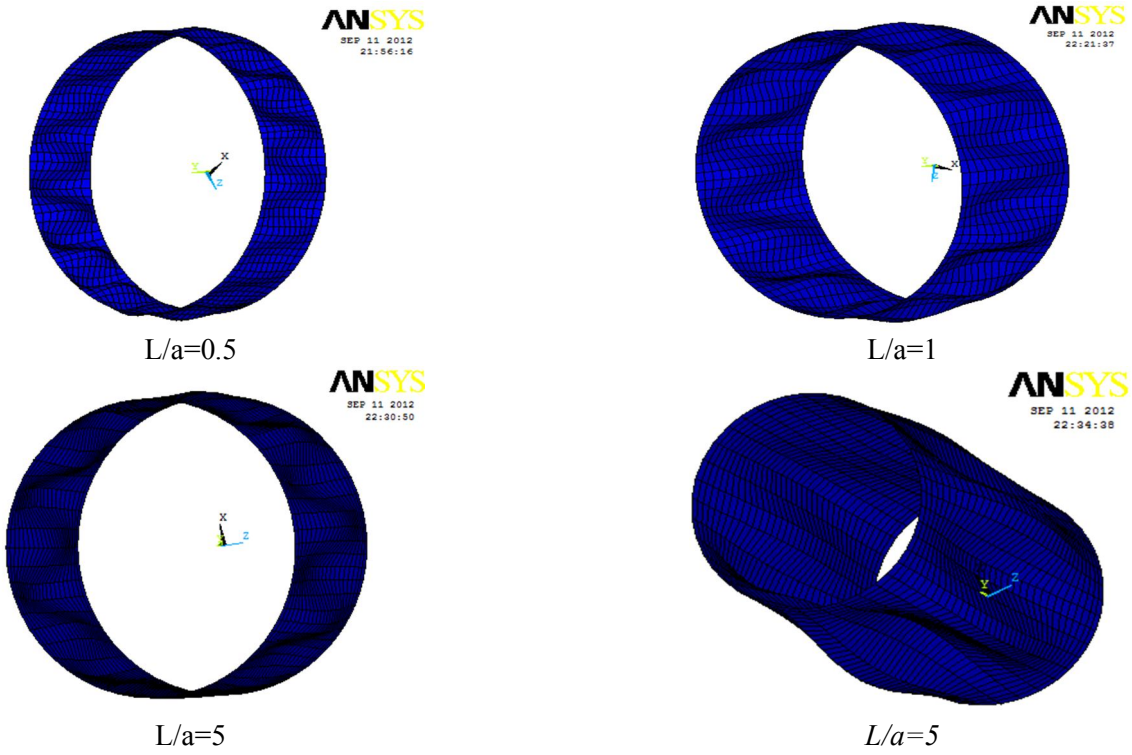

Figure 2. Buckling mode shapes for a thin complete shell

To study the accuracy of the present method against finite element solutions for thin and moderately thick shells, results for two cases of shells, i.e. a complete cylindrical shell and a curved panel with β=π/2 are shown in Table 3. It is clearly shown that two sets of results are in good agreement.

Table 3. Compare variation of buckling pressure (kPa) with geometric ratios

	Present		FEM	
a/h	β=360	β=90	β=360	β=90
10	7.83E+05	1.14E+06	8.69E+05	1.02E+06
12.5	4.38E+05	6.40E+05	4.73E+05	5.38E+05
20	1.13E+05	1.94E+08	1.40E+08	1.50E+05
30	3.47E+04	4.60E+04	3.77E+04	4.20E+04
100	2.08E+03	2.33E+03	2.33E+03	2.00E+03
200	3.50E+02	4.21E+02	4.11E+02	3.90E+02

Variation of critical loads with the curvature angle β for a moderately thick shell subjected to pure external pressure loading is presented in Figure 3. It is assumed that the panel is clamped at two side edges and simply supported at the upper and bottom edges. It is revealed from the figure that the critical load for higher values of β approaches an asymptotic value, i.e. the buckling load for a cylindrical shell

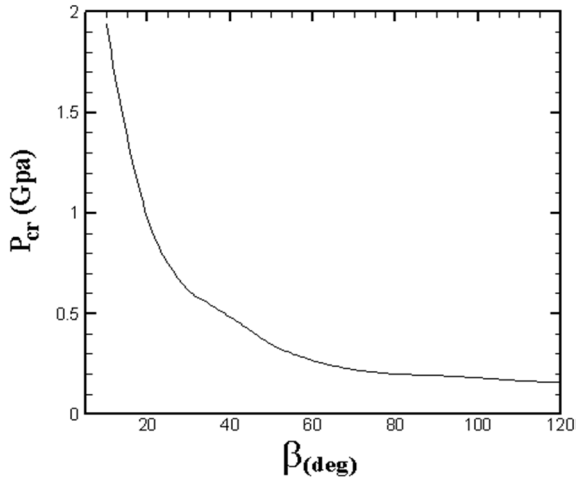

Figure 3. Variation of buckling pressure with curvature angle

The effect of the distance between ring stiffeners, i.e. the length of curved panel on its critical load for various curvature angles is shown in Figure 4. The panel is assumed to be subjected to uniform lateral pressure. It is realized from Figure 3 that as the value of L increases, the buckling load decreases and approaches to an asymptotic value. It is also revealed from this figure that buckling load variation is less sensitive to the length L of the panel with small curvature angel, β. In other word, as the number of straight stiffeners used for a cylindrical shell increases the dependency of local buckling pressure on the length or distance of ring stiffeners is reduced.

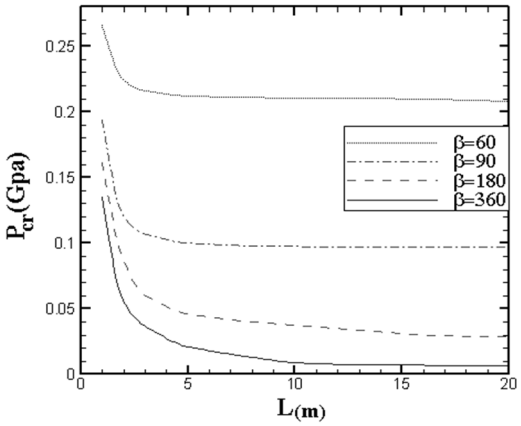

Figure 4. Variation of buckling pressure with length for different curved panels

To study the buckling behavior of a shell with imperfection, the quantity namely, λ denoting the ratio of the buckling load of the imperfect shell to that of the perfect shell is considered:

$$\lambda = \frac{P_{cr}^{(imper)}}{P_{cr}^{(per)}} \qquad (24)$$

The buckling load reduction parameter λ for pure external pressure loading cases of isotropic shells with *L/a*=1 and considering imperfection are presented in Figure 5. The results of this figure propose the same pattern as the one presented by Nguyen *et al*. [19].

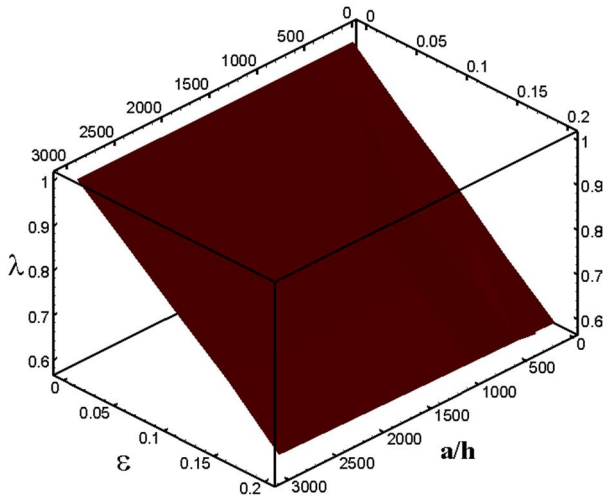

Figure 5. Variation of Buckling load reduction *λ* with *ε* and *a/h*

Next, results of the present method are compared with results obtained by classification societies rules requirements. A complete thin cylindrical shell subjected to pure external pressure loading is considered. Variation of buckling pressures obtained by the present method for different values of *a/h* and *L/a* are shown in Tables 4 and 5. Also the effect of the imperfection parameter on the buckling pressure of these shells is considered. It is evident from these tables that DNV and ABS rules present high factor of safety, especially for thin and long shells. Imperfections can reduce the buckling pressure significantly. It can be found that the buckling load ratio, *i.e.* the ratio of the buckling load of the imperfect shell to the perfect shell reduces linearly for small values of the imperfection factor. As shown in tables, for small values of *a/h* and *L/a*, the ABS rule gives lower value of the factor of safety for the design of imperfect cylindrical shells.

Table 4. Variation of buckling pressure (KPa) with *a/h* for thin shell under pure lateral pressure

	a/h	100	200	300	500	800	1000
FEM		2334	411.3	159.77	43.67	12.7	8.04
Present	ε=0	2089	374.8	175.03	54.48	17.9	10.45
	ε=0.05	1921.9	343	158.7	49	16.27	9.4
	ε=0.1	1692.1	307.7	142.1	43.58	14.48	8.4
	ε=0.15	1483.2	273.6	122.5	38.14	12.6	7.42
ABS		1667	283.6	101.3	27.79	8.5	4.8
(ABS/Present)*100		79.8	75.66	58	51	47.5	46
DNV		856.5	144.1	51.63	14.12	4.3	2.45
(DNV/Present)*100		41	38.4	29.5	26	24	23.4

Table 5. Variation of buckling pressure (KPa) with *L/a* , *a/h*=200 under pure lateral pressure

	L/a	1	2	3	5	10	20
Present	ε=0	374.8	187.6	129.7	81.1	41.2	23.3
	ε=0.05	343	177	117.38	73.64	37.08	20.78
	ε=0.1	307.7	152.3	104.64	65.37	32.96	18.54
	ε=0.15	273.6	134.1	90.92	56.93	28.84	16.15
ABS		283.6	135.7	89.24	52.29	24.36	11.63
(ABS/Present)*100		75.66	72.33	68.6	64.6	59.1	50
DNV		144.1	68.3	45.04	26.86	13.4	6.7
(DNV/Present)*100		38.4	36.4	34.72	33.1	32.5	28.8

Buckling loads for thin curved panels between adjacent pairs of ring and stringers stiffeners with *β=π/2* are listed in Table 6 and compared with results obtained by DNV rules. It is evident from this table that for curve panels as the imperfection parameter increases, the buckling load ratio reduces linearly as shown in figure 5.

Table 6. Variation of critical pressure (KPa) with *a/h* for curved panel with *L/a*=1and *β=π/2*

	a/h	100	200	300	500	800	1000
Present	ε=0	2329	421.2	193	65	17.37	11.2
	ε=0.05	2142.7	386.2	177.7	59.5	15.8	10.3
	ε=0.1	1909.8	343.53	156.3	53.1	14.2	9.1
	ε=0.15	1653.6	307.5	140	47.1	12.5	8.2
DNV		829	139.8	53.4	14.38	3.82	2.47
(DNV/Present)*100		35.6	33.2	27.7	22.1	22	22

For the axial loading case, variation of critical forces for a thin shell, with the ratio of *a/h* are presented in Table 7. The effect of the initial imperfection is also

considered. The results are compared with referred design rules. It can be observed from this table that the safety factor given by presented rules are higher for the axial loading case in comparison with that for the pure external pressure loading. It is shown that as the imperfection parameter ε increases, buckling load reduces and this reduction is smaller than the external pressure loading case. The results for the critical axial force of curved panels for different values of panel width are given in Table 8.

Table 8. Variation of buckling axial force (KN) with *s* for curved panel with *L/a*=2 and *h=0.003 mm*

s(m)	0.3	0.4	0.5	0.7	0.8	1
FEM	404	472	561	709	750	823
Present	368	425	528	667	722	795
ABS	119.35	147.53	177.46	236.2	265.7	324.3
DNV	65	78.7	95.17	130.8	149.1	186

Table 7. Variation of buckling force (KN) with *a/h* for thin shell under axial compression

	a/h	100	200	300	500	800	1000
Present	ε=0	67824	19386.3	8702.6	3136.9	980.6	784.5
	ε=0.05	67484	19172.7	8624.3	3130.6	969.8	778.2
	ε=0.1	65789	18901.6	8511.1	3074.1	960	964.1
	ε=0.15	65111	18707.8	8415.4	3042.8	944.3	946.1
ABS		10569.4	4515.5	2435.4	759.9	225.6	141
(ABS/Present)*100		15.6	23.3	28	24.2	23	14.5
DNV		7797.6	3008	1448.5	482.3	160.7	94
(DNV/Present)*100		11.5	15.5	16.6	15.4	16.4	12

6. Conclusions

In this paper, a set of stability equations of cylindrical shells and panels related to marine structures are obtained using three-dimensional elasticity theory. The resulting differential equations are discretized and solved by differential quadrature method. Buckling analysis of cylindrical shells and panels under the action of different types of mechanical loadings is carried out. It is assumed that curved panels bounded by adjacent pairs of rings and stiffeners have simply supported boundary condition at all panel edges. Effects of the curvature angles, shell geometric parameters, initial imperfection and loading conditions on the buckling behavior of these structures are investigated. Numerical results for buckling loads of thin and cylindrical shells are presented and compared with classification rules of ABS and DNV classification societies. It is shown that the requirements set by DNV is more conservative and provides higher factor of safety in comparison with ABS in designing marine and offshore structures.

7. Reference

1. A Ricles, J. M. and Hebor, M., (1999), *Structural testing of corroded offshore tubular members*, International Workshop on Corrosion Control for Marine Structures and Pipelines, Galveston, Texas, USA.

2. P. K, Das., Thavalingam, A. and Bai, Y., (2003), *Buckling and ultimate strength criteria of stiffened shells under combined loading for reliability analysis*, Thin-Walled Structures, Vol. 41,p. 69-88.

3. ABS Rules for Building and Classing Offshore Installations, (2011).

4. ABS Rules for Building and Classing Mobile Offshore Drilling Units, (2012).

5. ABS Rules for Building and Classing Steel Vessels, (2012).

6. Mirfakhraei, P., Huang, D., Redekop, D. and Xu, B., (1998), *Storage tanks under seismic loading-a bibliography, (1990-1996),* In: Proceedings of the 4th Mechanical Engineering Conference, Shiraz, Iran, ISME, P. 989-996, 1996.

7. Huang, D., Redekop, D., and Xu, B., (1996), *Instability of a cylindrical shell under three-point bending, Thin-walled Structures*, Vol. 26, p. 105-122.

8. Mirfakhraei, P., and Redekop, D., (1998), *Buckling of circular cylindrical shells by the differential quadrature method*, Int. J. pressure vessels and piping, Vol. 75, p. 347-353.

9. Shen, H-S., Chen, T-Y., (1990), *A boundary layer theory for the buckling of thin cylindrical shells under axial compression*, In: Chien WZ, Fu ZZ, editors. Advances in Applied Mathematics and Mechanics in China, vol. 2. Beijing, China: International Academic Publishers, p. 155–72.

10. Shen, H-S. and Chen, T-Y., (1988*), A boundary layer theory for the buckling of thin cylindrical shells under external pressure*, Applied Mathematics and Mechanics, Vol. 9, p.557-571.

11. Lai, W. M., and Rubin, D., and Krempl, E., (1996*), Introduction to Continuum Mechanics*, 3rd ed. Butterworth-Heinemann, Massachusetts.

12. Ciarlet, P. G., (1988), *Mathematical Elasticity, Vol. I, Three Dimensional Elasticity*. North-Holland: Amsterdam.

13. shu, C., (2000), *Differential quadrature and its application in Engineering, London*, Springer-Verlag.

14. DNV Rules for buckling strength of shells, (2010).

15. *ABS Rules for Buckling and ultimate strength assessment for offshore structures*, (2012).

16. Kardomateas, G. A., (1996), *Benchmark three-dimensional elasticity solution for the buckling of thick orthotropic cylindrical shells*, Journal Applied Mechanics, (ASME), Vol. 5, p.569.

17. Timoshenko, S. P., and Gere, J. M., (1961), *Theory of Elastic Stability*, McGraw Hill.

18. Flugge, W., (1960), *Stresses in shells*, Berlin, Heidelberg: Springer Verlag,

19. Nguyen, T.H.L., Elishakoff, I., Nguyen, T.V., (2009), *Buckling under external pressure of cylindrical shell with variable thickness*, Int. J. solids and structures, Vol. 46, p. 4163-4168.